Science Bulletin xxx (xxxx) xxx

Contents lists available at ScienceDirect

Science Bulletin

journal homepage: www.elsevier.com/locate/scib

Article

Current-reversion symmetry breaking and the DC Josephson diode effect

Da Wang [a,b,c,*], Qiang-Hua Wang [a,b], Congjun Wu [d,e,f,g,*]

[a] National Laboratory of Solid State Microstructures & School of Physics, Nanjing University, Nanjing 210093, China
[b] Collaborative Innovation Center of Advanced Microstructures, Nanjing University, Nanjing 210093, China
[c] Jiangsu Key Laboratory of Quantum Information Science and Technology, Nanjing University, China
[d] New Cornerstone Science Laboratory, Department of Physics, School of Science, Westlake University, Hangzhou 310024, China
[e] Institute for Theoretical Sciences, Westlake University, Hangzhou 310024, China
[f] Key Laboratory for Quantum Materials of Zhejiang Province, School of Science, Westlake University, Hangzhou 310024, China
[g] Institute of Natural Sciences, Westlake Institute for Advanced Study, Hangzhou 310024, China

ARTICLE INFO

Article history:
Received 14 May 2025
Received in revised form 3 August 2025
Accepted 27 October 2025
Available online xxxx

Keywords:
Josephson diode effect
Critical current
Current-reversion symmetry breaking
Particle-hole symmetry breaking

ABSTRACT

The direct-current (DC) Josephson, or superconducting diode effect, i.e., the nonreciprocal behavior of critical current in a superconductor, has been observed in various systems exhibiting both time-reversal and parity symmetry breakings. However, we show that breaking these two types of symmetries is only a necessary but not sufficient condition for the diode effect, for which certain additional symmetries, including particle-hole symmetry and many others, must also be broken. The dependencies of the free energy on the gauge-independent phase difference across the junction and the magnetic field are classified, exhibiting the current-reversion (JR), field-reversion, and field-current reversion conditions, respectively. All symmetries satisfying the JR condition need to be broken for the DC Josephson diode effect. The relations of critical currents with respect to the magnetic field are classified into five classes, and three of them exhibit the diode effect. These symmetry considerations are applied to concrete examples. Our work reveals that the DC Josephson diode effect is a natural consequence of the JR symmetry breaking, and hence provides a guiding principle to understand or design a DC Josephson diode.

1. Introduction

The semiconductor diode plays a fundamental role in modern electronics. Its superconducting analogies are the Josephson or superconducting diodes, including both the alternating-current (AC) and direct-current (DC) versions. The AC Josephson diode effect was first proposed by Hu, one of the authors, and Dai [1] in Josephson junctions between two superconductors that are hole-doped and electron-doped, respectively. This junction is Mott-insulating and plays the role of the depletion region. It shows nonreciprocal critical supercurrents with respect to the electric field across the junction, i.e., $J_c(E) \neq J_c(-E)$. On the other hand, the DC superconducting diode effect has been observed recently in many experiments at zero bias, exhibiting nonreciprocal critical current $|J_{c+}| \neq |J_{c-}|$ ($\pm$ labels the forward and backward directions) [2–21]. These advances have triggered a great deal of theoretical studies on the diode effect in superconductors [22–42].

We focus on the DC Josephson diode effect below. An important question is to figure out the conditions leading to such an effect. It is easy to recognize that all of time-reversal ($\mathcal{T}$) and parity symmetries, including inversion (I) and mirror reflection (M), have to be broken, since any of them protects $|J_{c+}| = |J_{c-}|$ [23–42]. For instance, in most experimental and theoretical studies, the DC superconducting diode effect for a current along the x-direction needs parity breaking with respect to the xz-plane and a magnetic field along the z-direction. However, one may still find various systems with all the above symmetries broken but still not exhibiting the diode effect. One example is the Josephson junction connecting two different materials (breaking I and M) with magnetic impurities in between (breaking $\mathcal{T}$), where the magnetic scattering would give rise to a π-junction [43] but does not exhibit the diode effect. Other examples will also be given in the text below. Therefore, except the easily distinguished $\mathcal{T}$, I and M breaking conditions, there still exist additional requirements to realize a DC Josephson, or superconducting, diode,

* Corresponding authors.
E-mail addresses: dawang@nju.edu.cn (D. Wang), wucongjun@westlake.edu.cn (C. Wu).

https://doi.org/10.1016/j.scib.2025.11.011

Please cite this article as: D. Wang, Q.-H. Wang and C. Wu, Current-reversion symmetry breaking and the DC Josephson diode effect, Science Bulletin, https://doi.org/10.1016/j.scib.2025.11.011

which goes beyond the usual setups. A unified picture, if it exists, is highly desired for future studies in this field.

In this article, we examine which symmetries forbid the DC Josephson diode effect, and hence all such symmetries have to be broken to realize such an effect. According to the even-or-odd dependence of the free energy with respect to the supercurrent $\boldsymbol{J}$ and magnetic field $\boldsymbol{B}$ reflections, there exist three relations, including current-reversion (JR), magnetic field-reversion (BR), and field-current reversion (BJR) ones. Any unitary or anti-unitary symmetry leading to the JR relation forbids the diode effect. The relations of critical current $J_{c\pm}$ with respect to the magnetic field $\boldsymbol{B}$ are classified into five classes, including three exhibiting the diode effect. Hamiltonians are constructed with the magnetic field and spin–orbit coupling (SOC) to examine the above relations, which reveal symmetry constraints more stringent than the previous time-reversal and parity ones. In particular, we find the particle-hole symmetry must also be broken to realize the diode effect, which has been overlooked in previous studies.

2. Current and field reversion conditions

We consider a Josephson junction with a superconducting phase difference $\Delta\phi$ across the junction. When the orbital effect of the magnetic field $\boldsymbol{B}$ needs to be considered, $\Delta\phi$ should be replaced by the gauge invariant version $\Delta\tilde{\phi} = \Delta\phi - (2e/\hbar)\int \mathbf{A}\cdot \mathrm{d}\ell$, where $\boldsymbol{A}$ is the vector potential to be integrated along the path across the junction. In addition, $\boldsymbol{B}$ also breaks $\mathcal{T}$ in the spin channel and hence manifests in the free energy F as well. In the most generic case, the free energy F could exhibit no symmetry with respect to $\boldsymbol{B}$ and $\Delta\tilde{\phi}$. Nevertheless, the experiment system may exhibit certain symmetries leading to the following relations,

$$\text{JR}: \quad F(\mathbf{B},\Delta\tilde{\phi}) = F(\mathbf{B},-\Delta\tilde{\phi}+\theta), \tag{1}$$

$$\text{BR}: \quad F(\mathbf{B},\Delta\tilde{\phi}) = F(-\mathbf{B},\Delta\tilde{\phi}+\theta), \tag{2}$$

$$\text{BJR}: \quad F(\mathbf{B},\Delta\tilde{\phi}) = F(-\mathbf{B},-\Delta\tilde{\phi}+\theta), \tag{3}$$

where θ is a constant global phase. Eqs. (1), (2), and (3) are termed as JR, BR, and BJR relations, respectively.

The above free energy conditions give rise to different symmetry relations of the critical supercurrents. The supercurrent is defined as $J = (2e/\hbar)\partial F/\partial\Delta\tilde{\phi}$, and the critical supercurrents $J_{c\pm}$ are maximal currents in the forward and backward directions, respectively. The following convention is assumed that $J_{c+} > 0$ and $J_{c-} < 0$. Eq. (1) leads to

$$\text{JR}: \quad J_{c+}(\mathbf{B}) = -J_{c-}(\mathbf{B}), \tag{4}$$

which protects the absence of the diode effect. In contrast, Eqs. (2) and (3) give rise to

$$\text{BR}: \quad J_{c\pm}(\mathbf{B}) = J_{c\pm}(-\mathbf{B}), \tag{5}$$

$$\text{BJR}: \quad J_{c+}(\mathbf{B}) = -J_{c-}(-\mathbf{B}). \tag{6}$$

In both cases, the Josephson diode effect appears if the JR relation is violated. Here, as a general result, an anharmonic phase-dependence of the free energy (supercurrent) is found to be necessary to yield the diode effect [44]. If the free energy depends linearly on $\sin\phi$ and $\cos\phi$, the JR condition Eq. (1) can always be satisfied by shifting a suitable global phase θ for the superconducting order parameter.

If any two of the above three conditions are satisfied, then the third one is automatically true. Hence, there exist five types: where all conditions, where one of the JR, BJR, and BR conditions, and where none are satisfied, as shown in Table 1. The former two situations show the absence of the diode effect, while the latter three exhibit it, labeled by type-I, II, III, respectively. For the type-I diode, the curves of $J_{c\pm}$ versus $\boldsymbol{B}$ are central symmetric, i.e., satisfying Eq. (6), which is widely observed in many experiments [2–8,10–12,14–18]. As for the type-II diode, the BR condition protects $J_{c\pm}(\mathbf{B}) = J_{c\pm}(-\mathbf{B})$, which is reported in the InAs-junctions under a background magnetic field [3] and the $NbSe_2/Nb_3Br_8/NbSe_2$-junctions [13] under zero external magnetic field.

We next analyze concrete symmetries leading to the above free energy conditions. As an example, a unitary symmetry U, or an anti-unitary symmetry $U\mathcal{K}$ ($\mathcal{K}$ the complex conjugate) leading to the JR relation can be expressed as

$$U^\dagger H(\mathbf{B},\Delta\tilde{\phi})U = H(\mathbf{B},-\Delta\tilde{\phi}+\theta), \tag{7}$$

or

$$U^\dagger H^*(\mathbf{B},\Delta\tilde{\phi})U = H(\mathbf{B},-\Delta\tilde{\phi}+\theta). \tag{8}$$

Either one leads to Eq. (1) and in turn Eq. (4). Similarly, the BR and BJR symmetry conditions can be constructed. Here, Eqs. (7) and (8) give a unified, precise and powerful way to check whether a given symmetry operation is a JR symmetry, i.e., one that reverses the supercurrent. In previous studies [23–42], researchers only focused on time-reversal and parity-like (including inversion, mirror and rotation) spatial symmetries. Instead, our method enables us to identify some unrecognized JR symmetries before, as shown below. Moreover, by further analyzing BR and BJR symmetries, we classify the diode effect into three classes for the first time.

For the type-I diode effect, we consider two typical configurations, i.e., $\boldsymbol{B}$ is parallel and perpendicular to $\mathbf{J}$, respectively. When they are parallel, e.g., $\mathbf{B}\|\mathbf{J}\|\hat{\mathbf{x}}$, the 2-fold rotation symmetries along the $\hat{\mathbf{y}}$ and $\hat{\mathbf{z}}$-axes (C_{2y}, C_{2z}) satisfy Eq. (7), while $\mathcal{T}$ and the combination of $\mathcal{T}$ with the 2-fold rotation around the $\hat{\mathbf{x}}$-axis, $\mathcal{T}C_{2x}$, satisfy Eq. (8). In either case, we arrive at the BJR condition of Eq. (3), which leads to the central symmetry of the curves of $J_{c\pm}$ versus $\boldsymbol{B}$ described by Eq. (6). On the other hand, the curves of $J_{c\pm}$ violate the reflection symmetries, indicating the Hamiltonian should break all of the following symmetries leading to BR and JR conditions, including inversion I, mirror reflections with respect to the yz, xz, and xy-planes (M_i with $i = x, y, z$), and the combined symmetries of $\mathcal{T}I, \mathcal{T}M_i$ ($i = x, y, z$), etc. If the field and the current are perpendicular, e.g., $\mathbf{J}\|\hat{\mathbf{x}}$ and $\mathbf{B}\|\hat{\mathbf{y}}$, similar conclusions can be drawn. Any one of the following symmetries, $\mathcal{T}, M_x, C_{2z}, \mathcal{T}M_y$, is sufficient to lead to the BJR condition. Conversely, all the following symmetries leading to BR and JR should be broken, $I, M_z, C_{2x}, C_{2y}, \mathcal{T}I, \mathcal{T}M_z, \mathcal{T}M_z$, and $\mathcal{T}C_{2y}$, etc.

Similar analysis can be straightforwardly applied to other situations, including the type-II and type-III diode effects, and also for the other two cases exhibiting no diode effect, as summarized in Table 1. The symmetry patterns are much richer than previous results in literature. They provide important guidance to design DC Josephson, or superconducting, diodes in future studies.

3. 1D model and the DC Josephson diode effect

We proceed to consider concrete models to verify the above symmetry conditions of the critical supercurrents. We first consider a superconducting chain along the $\hat{\mathbf{x}}$-axis as shown in Fig. 1a. The model Bogoliubov-de Gennes (BdG) mean-field Hamiltonian reads,

$$H_{1D} = \sum_i \left[c_i^\dagger(t_i + i\lambda_i\sigma_z)c_{i+1} + h.c.\right] + \sum_i c_i^\dagger(-\mu - \mathbf{B}\cdot\boldsymbol{\sigma})c_i + \left(\Delta_i c_{i\uparrow}^\dagger c_{i\downarrow}^\dagger + h.c.\right), \tag{9}$$

where c_i is a two-component spinor, $t_i = t$ is the nearest neighbor hopping inside two leads taken as the energy unit, and $t_i = \kappa t$ on the interface bond, μ is the chemical potential, Δ_i is the spin-

Table 1
Usual time-reversal and spatial symmetry constraints (with respect to the case of $\mathbf{B}=\mathbf{0}$) for the five classes of DC Josephson junctions. Without loss of generality, we assume the current $\mathbf{J}$ along the $\hat{\mathbf{x}}$-direction and the magnetic field $\boldsymbol{B}$ along $\hat{\mathbf{x}}$- or $\hat{\mathbf{y}}$-directions. For each case, we list the symmetries to be all broken, and the symmetries to be satisfied at least one.

		DC diode effect			Absence of DC diode effect	
		BJR (type-I)	BR (type-II)	None (type-III)	JR & BR & BJR	JR
	Sketches of $J_{c\pm}(B)$	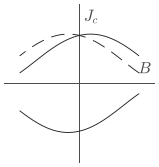	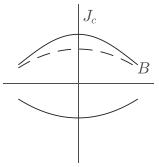	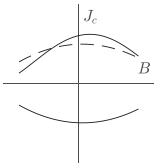	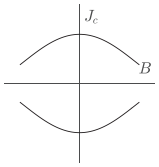	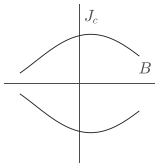
$\mathbf{J}\|\hat{\mathbf{x}},\mathbf{B}\|\hat{\mathbf{x}}$	Broken symmetries	$I, M_{x,y,z}, I\mathcal{T}, \mathcal{T}M_{x,y,z}$, etc.	$\mathcal{T}, I, M_x, C_{2y,2z}, \mathcal{T}M_{y,z}, \mathcal{T}C_{2x}$, etc.	$\mathcal{T}, I, M_{x,y,z}, C_{2y,2z}, \mathcal{T}M_{x,y,z}, \mathcal{T}C_{2x}, I\mathcal{T}$, etc.	none	$\mathcal{T}, M_{y,z}, C_{2y,2z}, I\mathcal{T}, \mathcal{T}C_{2x}, \mathcal{T}M_x$, etc.
	Satisfied symmetries	$\mathcal{T}, C_{2y,2z}, \mathcal{T}C_{2x}$, etc.	$M_{y,z}, I\mathcal{T}, \mathcal{T}M_x$, etc.	none	$(I,\mathcal{T}), (I, C_{2y,2z}), (\mathcal{T}, M_x)$, etc.	$I, M_x, \mathcal{T}M_{y,z}$, etc.
$\mathbf{J}\|\hat{\mathbf{x}},\mathbf{B}\|\hat{\mathbf{y}}$	Broken symmetries	$I, M_z, C_{2x,2y}, I\mathcal{T}, \mathcal{T}M_z, \mathcal{T}C_{2x,2y}$, etc.	$I, \mathcal{T}, M_x, C_{2y,2z}, \mathcal{T}M_{y,z}, \mathcal{T}C_{2x}$, etc.	$I, \mathcal{T}, M_{x,z}, C_{2x,2y,2z}, \mathcal{T}M_{y,z}, \mathcal{T}C_{2x,2y}, I\mathcal{T}$, etc.	none	$\mathcal{T}, M_{x,z}, C_{2x,2z}, I\mathcal{T}, \mathcal{T}M_y, \mathcal{T}C_{2y}$, etc.
	Satisfied symmetries	$\mathcal{T}, M_x, C_{2z}, \mathcal{T}M_y$, etc.	$M_z, C_{2x}, I\mathcal{T}, \mathcal{T}C_{2y}$, etc.	none	$(I,\mathcal{T}), (I, M_x), (I, C_{2y,2z})$, etc.	$I, C_{2y}, \mathcal{T}M_z, \mathcal{T}C_{2x}$, etc.

The abbreviation JR, BR, BJR stands for current/magnetic-field/magnetic-field&current reversion symmetries, as defined by Eqs. (1)–(3), respectively. The symbols $\mathcal{T}, I, M_i$ and C_{2i} $(i=x,y,z)$ denote time-reversal, space-inversion, mirror (normal to i-direction) and π-rotation (about i-axis), respectively. In the table, "none" means no relevant symmetries (as appearing in this table) for that case. These lists are incomplete. There may exist other symmetries denoted as "etc." in each list, such as complex conjugation, charge conjugation, and spin rotations (see examples in the main text).

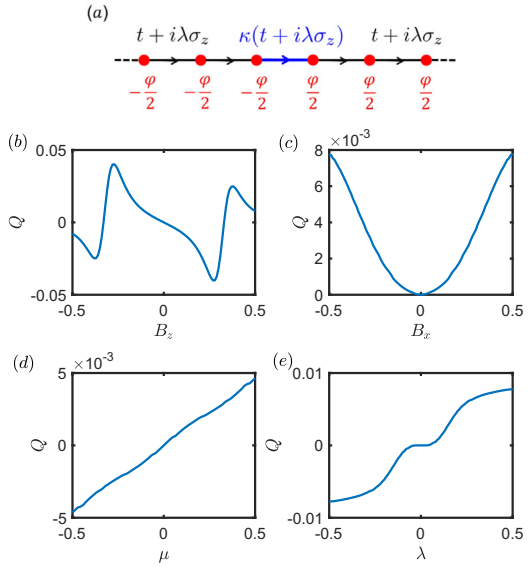

Fig. 1. (a) Scheme of the superconducting chain along $\hat{\mathbf{x}}$-direction. The hopping amplitude t and the SOC strength λ are reduced by a factor κ on the interface (blue) bond. The superconducting phases on the two leads are $\pm\varphi/2$. In numerical calculations, the length of each lead is set to 64 lattice sites. From (b) to (e), the nonreciprocal factor Q defined in Eq. (10) is plotted with varying B_z, B_x, μ and λ, respectively, while keeping the others fixed at $B_z = B_x = \lambda = 0.5, \mu = 1, \Delta = 0.2$ and $\kappa = 0.4$.

singlet pairing with phases $\pm\frac{\varphi}{2}$ on two sides, respectively. The Zeeman field $\boldsymbol{B}$ lies in the xz-plane. To avoid confusion, the Zeeman field can be either external (magnetic field) or internal (such as magnetic moment). In the following, we always take one component of $\boldsymbol{B}$ as arising from the external magnetic field, while keeping the others as internal. The SOC quantization axis lies along the $\hat{\mathbf{z}}$-axis, with the strength $\lambda_i = \lambda$ inside two leads and $\kappa\lambda$ on the interface bond. The Hamiltonian matrix can be numerically diagonalized to obtain the quasiparticle energy spectra E_n, which are then used to calculate the free energy F as a function of $\Delta\phi = \varphi$. Then, the Josephson current is obtained as $J(\varphi) = (2e/\hbar)\partial_\varphi F$, whose maximal/minimal values by varying φ give $J_{c\pm}$, respectively. More technical details can be found in the Supplemental material.

Such a system breaks the inversion symmetry by the SOC term and time-reversal symmetry by the Zeeman term, respectively. Hence, naively one would expect a DC Josephson diode effect. However, it only appears when all the quantities of λ, B_z, B_x, and μ are simultaneously nonzero. In Fig. 1b–e, the calculation of the nonreciprocal factor Q, defined as

$$Q = \frac{|J_{c+}| - |J_{c-}|}{|J_{c+}| + |J_{c-}|}$$

is plotted with varying each of the parameters B_z, B_x, μ and λ, while fixing the others at nonzero values. The above results show that as long as one of the parameters becomes zero, the DC Josephson diode effect vanishes because at least one symmetry survives leading to the JR condition of Eq. (1). The JR symmetries for the model Eq. (9) are explained below:

(I) If $\lambda = 0$, the inversion I is a unitary symmetry satisfying the JR condition, i.e., leaving the Hamiltonian invariant but reversing the supercurrent.

(II) If $B_z = 0$, the JR relation is satisfied due to the mirror reflection symmetry M_x. After turning on B_z, the JR condition is violated, and the M_x operation reverses the direction of B_z satisfying the BJR condition, giving the type-I (BJR) diode effect in Table 1. Here, we take B_z as the external magnetic field and B_x as the internal Zeeman field. The situations of $B_x = 0$ or $\mu = 0$ involve new symmetries not shown in Table 1 explained below.

(III) For $B_x = 0$, we first define a spin-twist operation U_{tw} as a position-dependent spin rotation

$$U_{\text{tw}} = \prod_i U(i), \tag{11}$$

with $U(i) = e^{i\frac{\sigma_z(i)}{2}(i-1)\eta}$ acting on site-i and $\eta = \arctan(\lambda_z/t)$. The spin twist leaves the B_z term unchanged, eliminates the SOC term, and transforms it into the hopping term by replacing t with $\sqrt{t^2+\lambda^2}$ in Eq. (9). Since the pairing is spin-singlet, it is not changed by this spin rotation. Then a combined operation $U = U_{\text{tw}} I U_{\text{tw}}^\dagger$ leaves the Hamiltonian invariant except switching the current direction. For spin-triplet superconductivity, there is no such a JR symmetry, as shown in the Supplemental material. For nonzero B_x, the π-

rotation in the spin space $R_z(\pi)=e^{i\frac{\pi}{2}\sigma_z}$ brings B_x to $-B_x$ without reflecting the current, satisfying the BR condition and hence the diode effect belongs to type-II (BR) in Table 1 by taking B_x as the external magnetic field.

(IV) For $\mu=0$, the particle-hole transformation $c_i\to(-1)^i\sigma_y c_i^\dagger$, brings $H(\Delta_i)$ to $H(-\Delta_i^*)$, hence, reversing the supercurrent as a result of the charge conjugation. Therefore, particle-hole symmetry satisfies the JR condition and must be broken to realize the diode effect. Although this exact particle-hole symmetry only applies to bipartite lattices at half-filling, it can be a good approximation when the energy band is near half-filling or in multi-band superconductors with mixed electrons and holes. For these systems, tuning the chemical potential (filling fraction) to enhance particle-hole asymmetry is expected to significantly amplify the diode effect.

4. 2D planer junction model with out-of-plane current

We next consider a bilayer model connected by a narrow junction schematically shown in Fig. 2a. The tunneling direction is along the $\hat{\mathbf{z}}$-direction. The BdG Hamiltonian reads

$$\begin{aligned}H_{2D}=&\sum_{n=t,b,\mathbf{k}}\{c_{n\mathbf{k}}^\dagger[\varepsilon_{\mathbf{k}}\sigma_0+\lambda_R(k_x\sigma_y-k_y\sigma_x)-\mathbf{B}\cdot\boldsymbol{\sigma}]c_{n\mathbf{k}}\\&+\left(c_{n\mathbf{k}\uparrow}^\dagger\Delta_n c_{n-\mathbf{k}\downarrow}^\dagger+h.c.\right)\}\\&+\sum_{\mathbf{k}}c_{t\mathbf{k}}^\dagger(t_z+i\lambda_z\sigma_z)c_{b\mathbf{k}}+h.c.,\end{aligned}\tag{12}$$

where t/b refers to the top/bottom layer; $\mathbf{k}=(k_x,k_y)$ is the in-plane momentum; t_z the tunneling matrix element. λ_R is the Rashba SOC, and λ_z is another SOC coupling to σ_z. The Zeeman field $\boldsymbol{B}$ is assumed to lie in the xz-plane. The spin-singlet pairings $\Delta_t=\Delta$ and $\Delta_b=\Delta e^{i\varphi}$, and then $\Delta\phi=\varphi$. The band dispersion is simply chosen as $\varepsilon_{\mathbf{k}}=-2t(\cos k_x+\cos k_y)-\mu$ with t taken as the energy unit. Similar

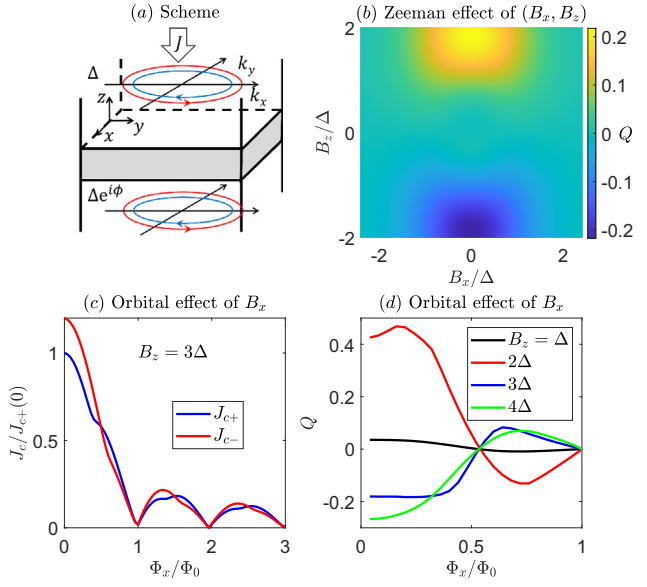

Fig. 2. (a) Scheme of the Josephson junction with the supercurrent along the $\hat{\mathbf{z}}$-direction. The Fermi surfaces are split due to the Rashba SOC and the spin directions are indicated by small arrows with different colors. (b) Shows the nonreciprocal factor Q versus B_x and B_z with only Zeeman effect considered. In (c) and (d), the orbital effect of B_x is taken into account, and the results of $J_{c\pm}$ and modified Q (see definition in the main text) with respect to Φ_x are given, respectively. In numerical calculations, we choose the parameters: $\Delta=0.2, \mu=3, \lambda_R=0.5, t_z=\lambda_z=0.4$.

to the 1D model, we diagonalize H_{2D} to calculate the free energy $F(\varphi)$, the Josephson current $J(\varphi)$, and extract $J_{c\pm}$ by varying φ subsequently.

The nonreciprocal factor Q is plotted on the (B_x,B_z) plane as shown in Fig. 2b. B_x itself cannot lead to a nonzero Q unless a nonzero B_z exists. Again, all the quantities of B_z,λ_z and λ_R need to be nonzero for the appearance of the diode effect. (I) If $B_z=0$, then the combined symmetry $\mathcal{T}C_{2z}$, leads to the JR condition and protects $Q=0$. For nonzero B_z, since $\mathcal{T}C_{2z}$ reflects B_z and current simultaneously, satisfying the BJR condition, the curves of $J_{c\pm}$ vs. B_z belongs to type-I (BJR) in Table 1. On the other hand, the B_x-dependence belongs to type-II (BR) in Table 1, since C_{2z} brings B_x to $-B_x$ satisfying the BR condition. (II) If $\lambda_z=0$, the combined symmetry $\mathcal{T}M_x$ leads to the JR condition and hence protects $Q=0$. (III) If $\lambda_R=0$, the symmetry satisfying the JR condition is a little subtle. We first perform a spin twist $U_{tw}=e^{-i\frac{\eta}{4}\sigma_{z,t}}e^{i\frac{\eta}{4}\sigma_{z,b}}$ with $\eta=\arctan(\lambda_z/t_z)$ to eliminate the λ_z-SOC term, which transforms $B_x\sigma_x$ to $B_x(\cos\frac{\eta}{2}\sigma_x\pm\sin\frac{\eta}{2}\sigma_y)$ ($\pm$ for top/bottom). Then we perform a $\frac{\pi}{2}$-rotation around σ_x, i.e., $R_x(\frac{\pi}{2})=e^{i\frac{\pi}{4}\sigma_x}$, to obtain $(B_x\cos\frac{\eta}{2}\sigma_x\pm B_z\sigma_y\mp B_x\sin\frac{\eta}{2}\sigma_z)$, which is invariant under the current-reflecting operation C_{2x}. At last, the above operations are inversely applied to recover the original Hamiltonian except $\Delta_n\to\Delta_n^*$. Putting them together, we obtain the combined JR symmetry $U=U_{tw}R_x(\frac{\pi}{2})C_{2x}R_x(-\frac{\pi}{2})U_{tw}^\dagger$ which protects $Q=0$.

We tentatively compare our results with the experiment on the $NbSe_2/Nb_3Br_8/NbSe_2$-junctions [13]. The DC Josephson diode effect is observed at zero external magnetic field and is suppressed by the in-plane field B_x, showing the type-II behavior in Table 1. According to the symmetry principle, the time-reversal must already be broken at $B_x=0$. It is then natural to conjecture the existence of a spontaneous ferromagnetic moment (still labeled by B_z for our convenience) [45,46]. This assumption may be at odds with the absence of longitudinal magnetoresistivity hysteresis with the $\hat{\mathbf{z}}$-directional external magnetic field [13], which deserves further studies. Another possibility for the $\mathcal{T}$-breaking is the pairing itself breaks time-reversal like in $s+id$ or $p+ip$ superconductors [29].

In our model, the λ_z-SOC term is necessary to cause the diode effect. This term requires M_z breaking, which is indeed possible since the interface Nb_3Br_8 does break M_z [47]. As a comparison, when the interface is replaced by few-layer graphene preserving M_z symmetry, the λ_z-term is forbidden, leading to absence of the (external) field-free diode effect [13]. In Fig. 2b, we find Q is evenly suppressed by B_x, qualitatively similar to the experiment, but the required field strength (of order $\Delta/\mu_B\sim 10$ T) is much larger than the experimental value ~ 10 mT [13]. This small field strength indicates that B_x should couple to J_z mainly through the orbital effect rather than the Zeeman effect. In this regard, we choose the vector potential $A_z=yB_x$ entering into t_z and λ_z through the Peierls phase $e^{i\pi(\Phi_x/\Phi_0)(y/L_y)}$, where $\Phi_0=h/2e$, and $\Phi_x=B_xL_yL_z$ is the total magnetic flux of B_x inserted into the junction with area $L_y\times L_z$. Within the quasiclassical picture, the supercurrent $J(\varphi,\Phi_{x,y})$ is integrated over y to obtain $J(\varphi,\Phi_x)$ and then $J_{c\pm}(\Phi_x)$. In Fig. 2c and d, $J_{c\pm}$ and the modified nonreciprocal factor $Q=[J_{c+}(\Phi_x)+J_{c-}(\Phi_x)]/[J_{c+}(0)-J_{c-}(0)]$ are plotted versus Φ_x, displaying a modulated nonreciprocal Fraunhofer pattern. The feature at small field with weak Φ_x-dependence is similar to the experimental results [13].

5. Summary

In summary, we have specified three types of symmetry conditions, i.e., JR, BR and BJR, based on which the relations of $J_{c\pm}$ vs. $\boldsymbol{B}$ are classified into five classes, including three exhibiting the DC Josephson diode effect. These symmetry constraints provide a uni-

fied picture to understand or design a DC Josephson diode in future studies.

Our theory provides a fundamental understanding of the DC Josephson diode effect. In fact, it essentially constitutes a no-go theorem, which states that the DC Josephson diode effect is forbidden by many symmetries (not only $\mathcal{T}, I$, but also particle-hole symmetry and many others as shown in the main text) collectively called JR symmetries in this work. Similar analysis can be applied to many other cases such as spin-triplet, chiral and Fulde-Ferrell-Larkin-Ovchinnikov superconductors with different geometries and vortices. The existence of vortices breaks time-reversal symmetry and their spatial distribution could break other JR symmetries, giving rise to the diode effect. The effect of impurities can also be taken into account by analyzing the symmetries. For example, nonmagnetic impurities may break parity but do not break time-reversal, hence, do not lead to diode effect by themselves. On the other hand, although magnetic impurities break both time-reversal and parity, the diode effect may still not happen due to other JR symmetries such as $\mathcal{T}\sigma_y = \mathcal{K}$. This directly addresses the question raised in the introduction: why magnetic impurities in asymmetric Josephson junctions do not always lead to the diode effect. Finally, different from the intrinsic Josephson diode effect discussed in this paper, there is another type of extrinsic Josephson diode effect arising from the boundary condition changed by external current reversion, as pointed out very recently [48–50].

Conflict of interest

The authors declare that they have no conflict of interest.

Acknowledgements

Da Wang thanks Heng Wu, Xiaoxiang Xi for helpful discussions and also thanks San-Jun Zhang for early collaborations in this project. This work was supported by the National Key R&D Program of China (2022YFA1403201, 2024YFA1408100), and the National Natural Science Foundation of China (12234016, 12274205, 12374147, 92365203, 12174317). This work has also been supported by the New Cornerstone Science Foundation.

Author contributions

Congjun Wu conceived the project. Da Wang and Congjun Wu carried out the symmetry analysis. Da Wang carried out the model calculations. All authors contributed to scientific discussion and manuscript written.

Appendix A. Supplementary data

Supplementary data associated with this article can be found online at https://doi.org/10.1016/j.scib.2025.11.011.

References

[1] Hu J, Wu C, Dai X. Proposed design of a Josephson diode. Phys Rev Lett 2007;99:067004.
[2] Ando F, Miyasaka Y, Li T, et al. Observation of superconducting diode effect. Nature 2020;548:7821.
[3] Baumgartner C, Fuchs L, Costa A, et al. Supercurrent rectification and magnetochiral effects in symmetric Josephson junctions. Nat Nanotechnol 2022;17:39.
[4] Bauriedl L, Bauml C, Fuchs L, et al. Supercurrent diode effect and magnetochiral anisotropy in few-layer $NbSe_2$. Nat Commun 2022;13:4266.
[5] Diez-Merida J, Diez-Carlon A, Yang SY, et al. Symmetry-broken Josephson junctions and superconducting diodes in magic-angle twisted bilayer graphene. Nat Commun 2023;14:2396.
[6] Farrar LS, Nevill A, Lim ZJ, et al. Superconducting quantum interference in twisted van der Waals heterostructures. Nano Lett 2021;21:6725.
[7] Idzuchi H, Pientka F, Huang KF, et al. Unconventional supercurrent phase in Ising superconductor Josephson junction with atomically thin magnetic insulator. Nat Commun 2021;12:5332.
[8] Lin JX, Siriviboon P, Scammell HD, et al. Zero-field superconducting diode effect in small-twist-angle trilayer graphene. Nat Phys 2022;18:1221.
[9] Lyu YY, Jiang J, Wang YL, et al. Superconducting diode effect via conformal-mapped nanoholes. Nat Commun 2021;12:2703.
[10] Miyasaka Y, Kawarazaki R, Narita H, et al. Observation of nonreciprocal superconducting critical field. Appl Phys Express 2021;14:073003.
[11] Pal B, Chakraborty A, Sivakumar PK, et al. Josephson diode effect from Cooper pair momentum in a topological semimetal. Nat Phys 2022;18:1228.
[12] Yun J, Son S, Shin J, et al. Magnetic proximity-induced superconducting diode effect and infinite magnetoresistance in a van der Waals heterostructure. Phys Rev Res 2023;5:L022064.
[13] Wu H, Wang Y, Xu Y, et al. The field-free Josephson diode in a van der Waals heterostructure. Nature 2022;604:653.
[14] Hou Y, Nichele F, Chi H, et al. Ubiquitous superconducting diode effect in superconductor thin films. Phys Rev Lett 2023;131:027001.
[15] Golod T, Krasnov VM. Demonstration of a superconducting diode-with-memory, operational at zero magnetic field with switchable nonreciprocity. Nat Commun 2022;13:3658.
[16] Narita H, Ishizuka J, Kawarazaki R, et al. Field-free superconducting diode effect in noncentrosymmetric superconductor/ferromagnet multilayers. Nat Nanotechnol 2022;17:828.
[17] Gupta M, Graziano GV, Pendharkar M, et al. Gate-tunable superconducting diode effect in a three-terminal Josephson device. Nat Commun 2023;14:3078.
[18] Turini B, Salimian S, Carrega M, et al. Josephson diode effect in high-mobility InSb nanoflags. Nano Lett 2022;22:8502.
[19] Sato Y, Ueda K, Takeshige Y, et al. Quasiparticle trapping at vortices producing Josephson supercurrent enhancement. Phys Rev Lett 2022;128:207001.
[20] Zhu Y, Wang H, Wang Z, et al. Persistent Josephson tunneling between $Bi_2Sr_2CaCu_2O_{8+x}$ flakes twisted by 45° across the superconducting dome. Phys Rev B 2023;108:174508.
[21] Le T, Pan Z, Xu Z, et al. Superconducting diode effect and interference patterns in kagome CsV_3Sb_5. Nature 2024;630:64.
[22] Misaki K, Nagaosa N. Theory of the nonreciprocal Josephson effect. Phys Rev B 2021;103:245302.
[23] He JJ, Tanaka Y, Nagaosa N. A phenomenological theory of superconductor diodes. New J Phys 2022;24:053014.
[24] Yuan NFQ, Fu L. Supercurrent diode effect and finite-momentum superconductors. Proc Natl Acad Sci USA 2022;119. e2119548119.
[25] Daido A, Ikeda Y, Yanase Y. Intrinsic superconducting diode effect. Phys Rev Lett 2022;128:037001.
[26] Alidoust M, Shen C, Zutic I. Cubic spin-orbit coupling and anomalous Josephson effect in planar junctions. Phys Rev B 2021;103:L060503.
[27] Halterman K, Alidoust M, Smith R, et al. Supercurrent diode effect, spin torques, and robust zero-energy peak in planar half-metallic trilayers. Phys Rev B 2022;105:104508.
[28] Zhang Y, Gu Y, Li P, et al. General theory of Josephson diodes. Phys Rev X 2022;12:041013.
[29] Zinkl B, Hamamoto K, Sigrist M. Symmetry conditions for the superconducting diode effect in chiral superconductors. Phys Rev Res 2022;4:033167.
[30] Jiang J, Wang YL, Milosevic MV, et al. Reversible ratchet effects in a narrow superconducting ring. Phys Rev B 2021;103:014502.
[31] Scammell HD, Li JIA, Scheurer MS. Theory of zero-field superconducting diode effect in twisted trilayer graphene. 2D Mater 2022;9:025027.
[32] Davydova M, Prembabu S, Fu L. Universal Josephson diode effect. Sci Adv 2022;8:eabo0309.
[33] Zhai B, Li B, Wen Y, et al. Prediction of ferroelectric superconductors with reversible superconducting diode effect. Phys Rev B 2022;106:L140505.
[34] Karabassov T, Bobkova IV, Golubov AA, et al. Hybrid helical state and superconducting diode effect in superconductor/ferromagnet/topological insulator heterostructures. Phys Rev B 2022;106:224509.
[35] Souto RS, Leijnse M, Schrade C. Josephson diode effect in supercurrent interferometers. Phys Rev Lett 2022;129:267702.
[36] Legg HF, Loss D, Klinovaja J. Superconducting diode effect due to magnetochiral anisotropy in topological insulators and Rashba nanowires. Phys Rev B 2022;106:104501.
[37] Tanaka Y, Lu B, Nagaosa N. Theory of giant diode effect in d-wave superconductor junctions on the surface of a topological insulator. Phys Rev B 2022;106:214524.
[38] Jiang J, Milosevic MV, Wang YL, et al. Field-free superconducting diode in a magnetically nanostructured superconductor. Phys Rev Appl 2022;18:034064.
[39] Hu JX, Sun ZT, Xie YM, et al. Josephson diode effect induced by valley polarization in twisted bilayer graphene. Phys Rev Lett 2023;130:266003.
[40] Steiner JF, Melischek L, Trahms M, et al. Diode effects in current-biased Josephson junctions. Phys Rev Lett 2023;130:177002.
[41] Nakamura K, Daido A, Yanase Y. Orbital effect on the intrinsic superconducting diode effect. Phys Rev B 2024;109:094501.
[42] Volkov PA, Lantagne-Hurtubise E, Tummuru T, et al. Josephson diode effects in twisted nodal superconductors. Phys Rev B 2024;109:094518.
[43] Buzdin AI. Proximity effects in superconductor-ferromagnet heterostructures. Rev Mod Phys 2005;77:935.
[44] Fominov YV, Mikhailov DS. Asymmetric higher-harmonic SQUID as a Josephson diode. Phys Rev B 2022;106:134514.

[45] Zhu X, Guo Y, Cheng H, et al. Signature of coexistence of superconductivity and ferromagnetism in two-dimensional $NbSe_2$ triggered by surface molecular adsorption. Nat Commun 2016;7:11210.
[46] Wickramaratne D, Khmelevskyi S, Agterberg DF, et al. Ising superconductivity and magnetism in $NbSe_2$. Phys Rev X 2020;10:041003.
[47] Pasco CM, El Baggari I, Bianco E, et al. Tunable magnetic transition to a singlet ground state in a 2D van der Waals layered trimerized kagome magnet. ACS Nano 2019;13:9457.
[48] Shi X, Dou Z, Pan D, et al. Circuit-level-configurable zero-field superconducting diodes: a universal platform beyond intrinsic symmetry breaking. arXiv: 2505.18330; 2025.
[49] Nagata U, Aoki M, Daido A, et al. Field-free superconducting diode effect in layered superconductor FeSe. Phys Rev Lett 2025;134:236703.
[50] Wang D, Wang QH, Wu C. Josephson diode effect: a phenomenological perspective. arXiv: 2506.23200; 2025.